Association of Metallurgical Engineers of Serbia *Scientific paper*
AMES *UDC: 669.295.018:677.4*

FABRICATION AND CHARACTERIZATION OF TiAl/Ti_3Al-BASED INTERMETALLIC COMPOSITES (IMCS) REINFORCED WITH CERAMIC PARTICLES

V. Kevorkijan[1], S.D. Škapin[2]

[1]*Independent Researching plc, Betnavska cesta 6, 2000 Maribor, Slovenia, varuzan.kevorkijan@impol.si*
[2]*Institute Jozef Stefan, Jamova 39, 1000 Ljubljana, Slovenia*

Received 15.01.2009
Accepted 31.03.2009.

Abstract

Dense (>95% of theoretical density) TiAl and Ti_3Al based composites reinforced with 10-50 vol. % of B_4C, TiC or TiB_2 particles were successfully prepared by pressureless reaction sintering of reaction mixtures consisting of commercial titanium aluminide powders (TiAl and Ti_3Al) blended with the appropriate amount of ceramic reinforcement. The green compacts made from the blended powder mixture were reaction sintered at 1300 °C for 2 h in an Ar+4 vol. % H_2-rich environment using a vacuum furnace. The morphology of the commercial powders and the microstructure of the as-sintered composites were studied by SEM-EDS and X-ray diffraction analysis. The mechanical properties were measured by tensile tests performed at room temperature. In the case of reactive systems (TiAl-B_4C, TiAl-TiC and Ti_3Al-B_4C, Ti_3Al-TiC), densification proceeds via formation of various secondary bonding phases, whilst in non-reactive system (TiAl-TiB_2 and Ti_3Al-TiB_2) the process seems to proceed by diffusion in liquid state. Regarding the room temperature tensile properties of the composites, superior improvement was observed in TiAl-B_4C, TiAl-TiC and Ti_3Al-B_4C, Ti_3Al-TiC samples with 50 vol. % of ceramic particles. However, in TiAl-TiB_2 and Ti_3Al-TiB_2 samples the improvement was significantly lower, most probably due to the lack of chemical affinity between ceramic reinforcement and $TiAl_3$ matrix.

Key words: Aluminium titanates, reaction synthesis, intermetallic matrix composites (IMCs), ceramic particulate reinforcement, reaction sintering, metallographic characterization

Introduction

TiAl/Ti_3Al-based alloys have several advantages over conventional titanium alloys, such as higher elastic modulus, lower density, better mechanical properties at elevated temperatures, and higher oxidation resistance due to the formation of a surface-

passivated alumina layer [1,2]. TiAl/Ti_3Al intermetallic-matrix composites (IMCs) reinforced with ceramic particles generally possess even higher specific strength and specific stiffness, increased creep strength, improved toughness, and high-temperature strength retention [3, 4].

However, bringing these attractive intermetallic composite matrices into commercial use largely depends upon the availability of practical and competitive enough processing routes. Due to difficulties in their production by conventional methods and the high cost of powder processing, the elemental powder metallurgy (EPM) route has been gaining more and more attention because near-net shape titanium aluminide alloy products can be fabricated by the consolidation and forming of blended Ti and Al elemental powders, followed by a subsequent pressureless reactive synthesis and sintering process [5-11]. However, due to the large difference between the partial diffusion coefficients of Ti and Al and the immobility of Ti atoms towards Ti/Al solid state reaction, the synthesis of TiAl/Ti_3Al alloys via reactive sintering follows a mechanism in which Al atoms move into the Ti lattice, thus leading to the formation of Kirkendall diffusion pores [10, 12, 13]. Although hot isostatic pressing (HIP) and other pressure assisted methods have been reported to be effective in eliminating the porosity of reactively sintered TiAl/Ti_3Al alloys [14-19], the high cost and low production efficiency make it unsuitable for commercial use.

However, in the pressent study the assumption was made that the appearance of Kirkendall diffusion pores during pressureless sintering may be significantly reduced by replacing Ti and Al elemental powders with TiAl/Ti_3Al, previously synthesized via EPM.

Thus, the aim of this study (the first part of a research project) was to investigate the potential of the pressureless sintering method in fabrication of fully dense, high quality TiAl/Ti_3Al -based IMCs by applying reaction mixtures consisting of commercial titanium aluminide powders doped with various amounts (from 10 to 50 vol. %) of different ceramic particles (TiB_2, TiC, B_4C).

Ti-Al phase diagram

Examination of the Ti-Al phase diagram (Fig.1 [20]), shows the presence of the following compounds in this system; Ti_3Al (super alpha, α_2), TiAl (gamma, γ), $TiAl_2$ (delta, δ) and $TiAl_3$, and α-Ti, β-Ti and α-Al terminal solid solutions.

Ti_3Al has the tetragonal DO_{19} structure and TiAl has the hexagonal LI_0 structure (which is basically an fcc lattice with atomic ordering and tetragonal distortion). The trialuminide $TiAl_3$ crystallizes with the tetragonal DO_{22} structure.

For structural applications the near gamma ($\alpha_2+\gamma$) phase is more reliable. Near gamma titanium aluminides are classified into single and two phase Ti-(46-52) at% Al alloys. The single phase near gamma alloys exhibit a lamellar microstructure. On the other hand, the significant two phases near gamma alloy appears in two different structures depending on the aluminium content. In the case of Ti-(46-48) at% Al the structure is a nearly lamellar and a duplex for Ti-(49-52) at% Al. Nearly lamellar structures are defined as coarse lamellae grains with minor amounts of fine γ grains or gamma grains in the lamellar grain boundaries. The lamellar structure consists of alternating plates of the γ-TiAl and α_2-Ti_3Al phases. Such a lamellar structure results from the solid state phase transformation of the primary disordered α dendrites. The γ

regions surrounding the lamellar grains result from the transformation of the aluminium-rich interdendritic melt.

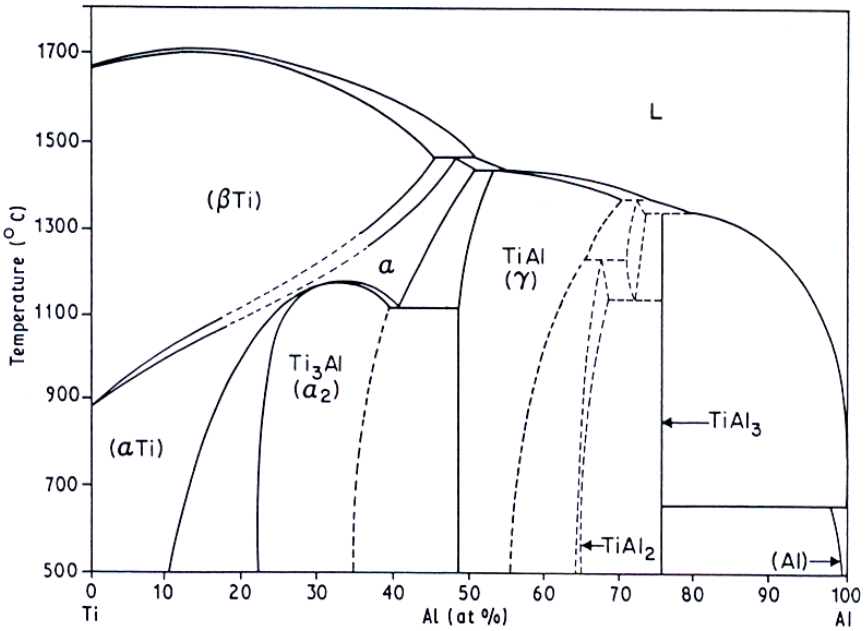

Fig.1. Schematic binary Ti-Al phase diagram [20].

Experimental

Composites were formulated by blending commercially available powders of either TiAl or Ti_3Al (technical grade with traces of Al and Ti) with ceramic powders (B_4C, TiC or TiB_2) in appropriate amounts to create titanium aluminide-based matrices with 10, 20, 30, 40 and 50 vol. % of B_4C, TiC or TiB_2 discontinuous reinforcement.

The powder blends were thoroughly mixed and subsequently cold compacted. In all cases, the reaction synthesis was conducted at 1300 °C for 2 h in an Ar+4 vol. % H_2-rich environment using a vacuum furnace. The as-synthesized composite samples were cut, machined and polished in accordance with standard procedures.

Microstructural characterization was performed by optical and scanning electron microscopy (OM and SEM, EDS), whereas X-ray diffraction (XRD) measurements were applied to the samples to identify the phases and their crystal structure.

The specimens for OM observation were electrolytically polished in a solution of 95% CH_3COOH and 5% $HClO_4$, and then etched in a solution of 5% HNO_3, 15% HF, and 80% H_2O. The main grain sizes were measured by the linear intercept method.

The specimens for XRD were abraded with SiC paper and were then subjected to diffraction using CuK_α radiation.

Quantitative determination of the volume percentage of ceramic particles in polished composite bars and the retained porosity was performed by analysing optical

and scanning electron micrographs of infiltrated composites using the point counting method and image analysis and processing software.

Composite density measurements were carried out in accordance with Archimedes' principle, applying distilled water as the immersion fluid. The initial density of the green compacts was calculated from the mass and geometry of the samples.

The tensile properties (ultimate tensile strength-UTS, 0.2% yield strength-YS and elongation) of the composite specimens were determined in accordance with the ASTM test method, E8M-96. The tensile tests were conducted on round tension-test specimens 3.5 mm in diameter and 16 mm gauge length using an automated servo-hydraulic tensile testing machine with a crosshead speed of 0.254mm/60 s.

Results and discussion

Morphology of titanium aluminide powders applied

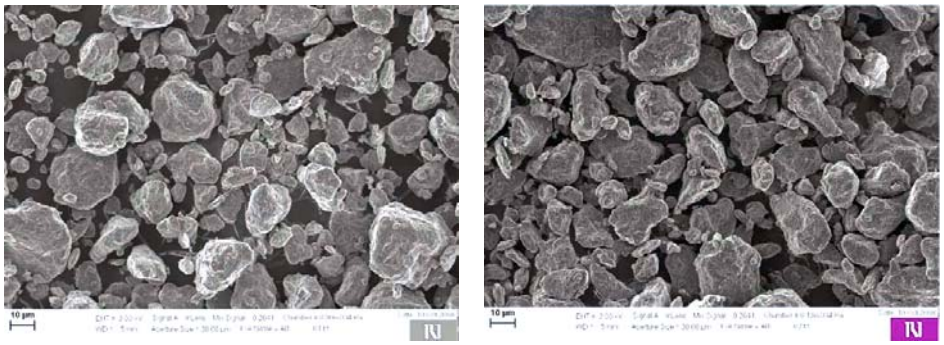

Fig. 2. SEM micrograph of as-received commercial TiAl powder.

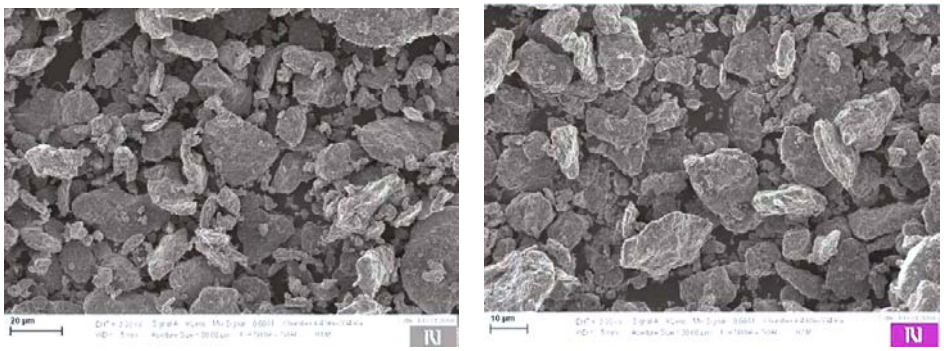

Fig. 3. SEM micrograph of as-received commercial Ti_3Al powder.

The morphology of TiAl and Ti_3Al powders are very similar. Both powders applied in this study were non-agglomerated, with well shaped individual particles. The

main difference is in the average particle size, which in the case of the as-received TiAl is about 12 μm and in the case of as-recived Ti_3Al is about 20 μm.

Microstructure development in IMCs

Generally, the microstructure of IMCs consists of an intermetallic matrix (based on an ordered intermetallic compound or a multiphase combination of intermetallic compounds), the ceramic particulate reinforcement and the interfacial region with secondary phases formed during reactive sintering.

Regarding the matrix itself, during the last three decades a large variety of titanium aluminide microstructures have been developed. The most promising microstructures are generally referred to as *fully-lamellar*, *nearly-lamellar* and *duplex*. The fully-lamellar microstructure consists of colonies (or grains) containing aligned platelets (lamellae) of γ-TiAl and α_2-Ti_3Al intermetallic phases [21]. In the case of the nearly-lamellar microstructure, the boundaries of γ-TiAl + α_2-Ti_3Al colonies, and, in particular, three-colony junctions are decorated with fine γ-TiAl grains [21]. The duplex microstructure consists of a mixture of equiaxial γ-TiAl grains and γ-TiAl + α_2-Ti_3Al colonies [21].

The microstructure of individual γ-TiAl+ α_2-Ti_3Al colonies consists of parallel γ-TiAl and α_2-Ti_3Al lamellae. The α_2-Ti_3Al phase is generally the minor phase whose volume fraction is typically less than 20 vol%. The β-phase particles are, in general, preferentially located at three-colony junctions [22].

SEM micrographs of various reactive sintered composite samples are shown in Figs. 4-15. A near-uniform distribution of the ceramic particulate reinforcements (B_4C, TiB_2 and TiC) through the both TiAl and Ti_3Al intermetallic matrices with no distinct evidence of clustering, or agglomeration is observed. This proves the effectiveness of the reactive sintering for producing composite microstructures.

In both TiAl and Ti_3Al intermetallic matrices, inclusions of Ti particles and solidified aluminium, were occasionally found. As a rule, in samples based on TiAl matrix, the traces of Ti_2Al_5, $TiAl_2$, Ti_5Al_{11} and Ti_9Al_{23} phases were observed. The suggested mechanism of the above phases formation is through a series of solid-liquid and/or solid state reactions necessarily involving TiAl as one of the starting phases [22].

An additional phase, frequently detected in both TiAl and Ti_3Al-based composites, is $TiAl_3$. This phase is formed during reactive sintering as the product of the reaction between solid Ti and liquid aluminium [22]:

$$Ti(s)+Al(l)=TiAl_3(s) \quad (1)$$

As reported by Sujata et al. [22], $TiAl_3$ is the only product of Reaction 1, because other possible products (TiAl and Ti_3Al) are with significantly higher free energies of formation.

B_4C-titanium aluminide (TiAl and Ti_3Al) system

Reactive sintering of B_4C-TiAl and B_4C-Ti_3Al composite samples resulted in specimens with densities higher than 95% of the theoretical density. In common with

densification, boron carbide particulate reinforcement reacted with intermetallic matrix forming secondary ceramic reinforcing phases (TiB_2, TiC, $Al_2Ti_4C_2$, Al_3BC), usually detected in sintered samples at the B_4C-matrix interface.

In the systems B_4C-Ti_3Al and B_4C-TiAl intensive chemical reactivity between the composite constituents was observed during high temperature densification due to the fact that boron carbide reacts with both molten aluminium and solid titanium [23, 24].

Boron carbide reacts at high temperature (1300 °C) with aluminium, forming mainly $AlB_{24}C_4/Al_4C_3$ and some AlB_{12} (Reaction 2):

$$21B_4C(s)+16Al(l)=3AlB_{24}C_4(s)+3Al_4C_3(s)+AlB_{12} \quad (2)$$

However, boron carbide also reacts with solid titanium particles producing secondary TiC and TiB_2:

$$B_4C(s)+3Ti(s)=2TiB_2(s)+TiC(s) \quad (3)$$

The possible overall stoichiometric reactions between boron carbide and particular titanium aluminides used in experimental work are the following:

$$32B_4C(s)+16Ti_3Al=32TiB_2(s)+16TiC(s)+3AlB_{24}C_4(s)+3Al_4C_3(s)+AlB_{12}(s) \quad (4)$$

$$79B_4C(s)+48TiAl=32TiB_2(s)+16TiC(s)+9AlB_{24}C_4(s)+9Al_4C_3(s)+3AlB_{12}(s) \quad (5)$$

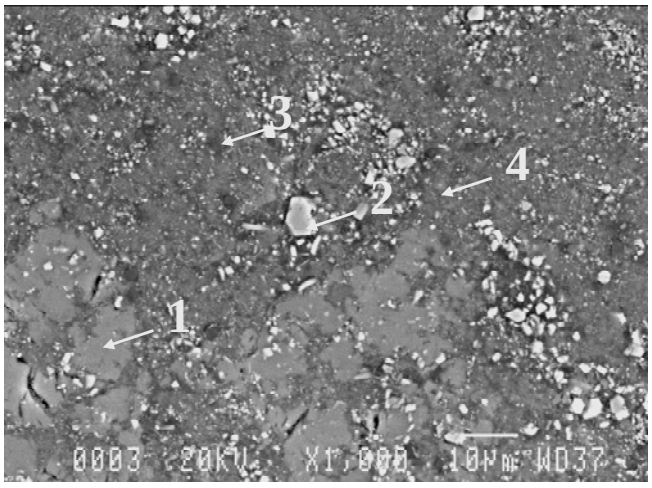

Fig. 4. SEM micrograph of fully dense TiAl -10% B_4C composite samples with (1) an TiAl alloy matrix (fine and equiaxed γ-TiAl with traces of Ti_2Al_5, $TiAl_2$, Ti_5Al_{11} and Ti_9Al_{23}), (2) TiB_2 bright grains, (3) TiC gray grains and (4) Al_3Ti gray phase in the matrix.

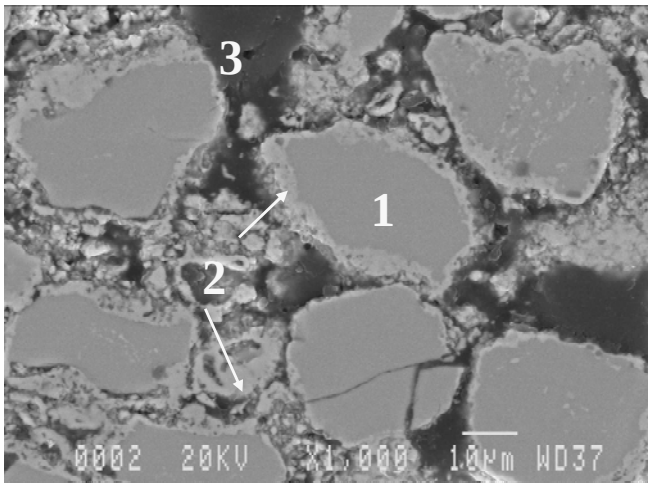

Fig. 5. SEM micrograph of a reactively sintered TiAl-10 vol. % B_4C composite showing different phases: (1) Al_3Ti, (2) TiB_2 and (3) $Al_2Ti_4C_2$.

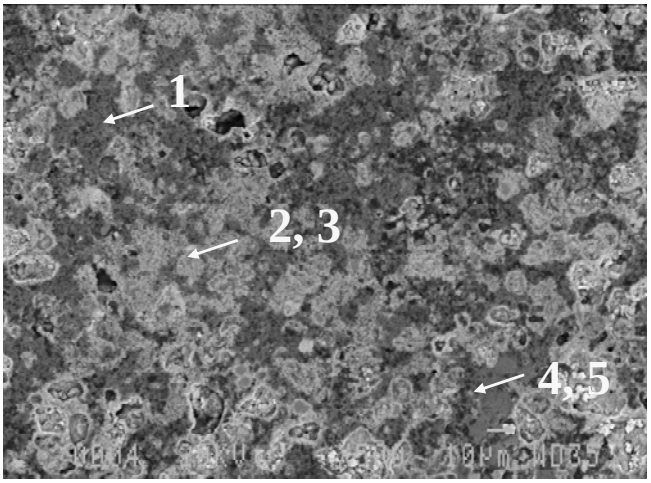

Fig. 6. Representative microstructures of a fully dense Ti_3Al-40 vol. % B_4C composite prepared by reactive sintering of Ti_3Al + 40 vol. % B_4C: (1) dark spots-B_4C, (2) and (3) bright phases-AlB_2 and TiB_2, (4) and (5) grey phases-Al and probably also Al_4C_3. In Ti_3Al matrix, traces of Al_3BC are also identified.

TiB_2-titanium aluminide (TiAl and Ti_3Al) system

TiB_2 is stable at 1300°C in contact with a TiAl and Ti_3Al matrix. The main microstructural features that can be varied in that case include the matrix grains morphology and distribution.

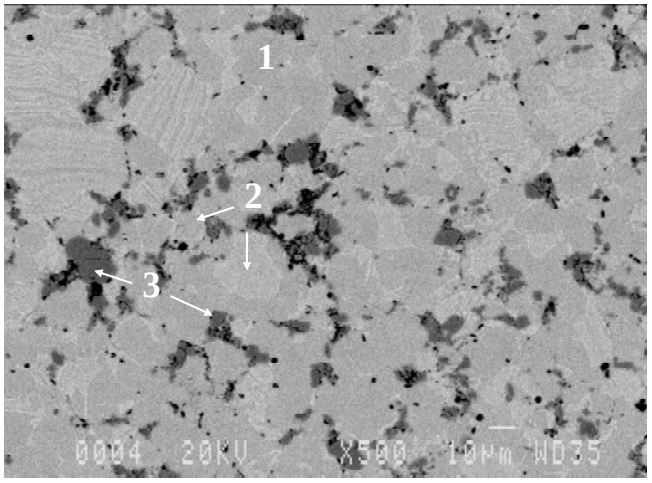

Fig. 7. Microstructure of TiAl-20 vol. %TiB_2 composite. The microstructural constituents are: (1) TiAl lamellae grey phase in the matrix with planar grain boundaries, (2) Ti_3Al grains in and (3) TiB_2 grains.

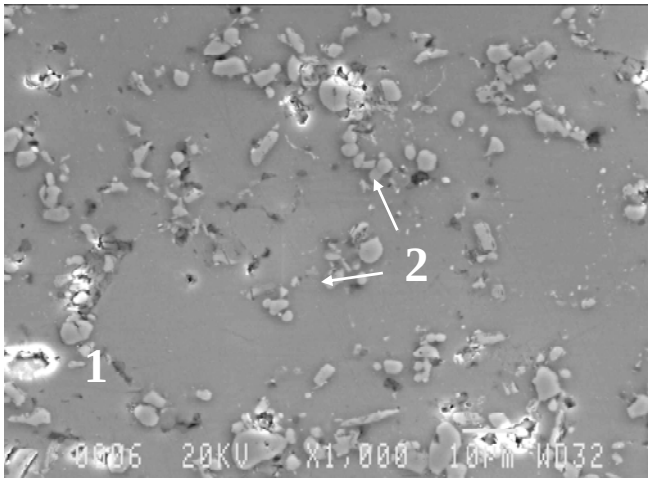

Fig. 8. Scanning electron micrographs of Ti_3Al-20 vol. % TiB_2 composite showing: (1) Al_3Ti in sintered Ti_3Al matrix reinforced with (2) TiB_2 grains.

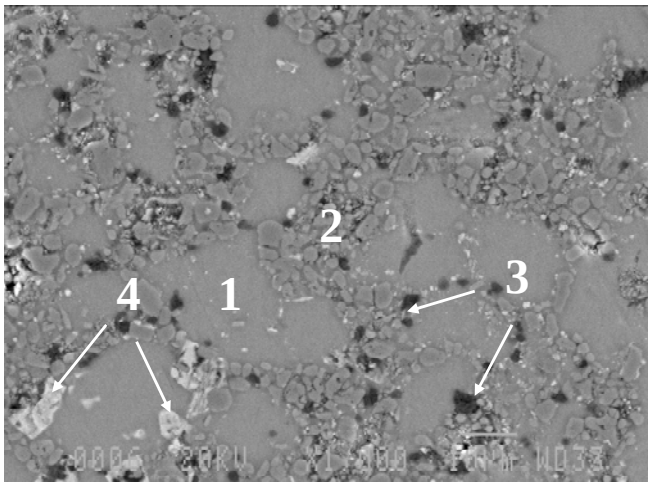

Fig. 9. Microstructure of a TiAl-30 vol. % TiB_2 composite showing different morphologies of the phases observed in the composite: (1) Al_3Ti grains in TiAl matrix, (2) TiB_2 grains, (3) Al_2O_3 dark inclusions and (4) traces of Ti_2Al_5, $TiAl_2$, Ti_5Al_{11} and Ti_9Al_{23}.

TiC-titanium aluminide (TiAl and Ti_3Al) system

In this system, the best sintering results were experimentally obtained. Almost all the sintered samples, including these with a high amount (50 vol. %) of ceramic reinforcement, had a retained porosity below 5 vol. %, beside which numerous were fully dense.

Regarding high temperature (1300°C) reactivity in TiAl-TiC and Ti_3Al samples, Ti_3AlC and Al_3C_3 phases are confirmed at the matrix-reinforcement interface, according to the following chemical reactions [25]:

$$9TiC_{(s)} + 11Al_{(l)} = 2Al_4C_{3(s)} + 3Ti_3AlC_{(s)} \quad (6)$$

or:

$$3TiC_{(s)} + 13Al_{(l)} = Al_4C_{3(s)} + 3Ti_3Al_{(s)} \quad (7)$$

Thereby, as in the case of the other reactive systems (TiAl-B_4C and Ti_3Al-B_4C) considered in this work, in TiAl-TiC and Ti_3Al-TiC, a variety of secondary microstructural features was also found.

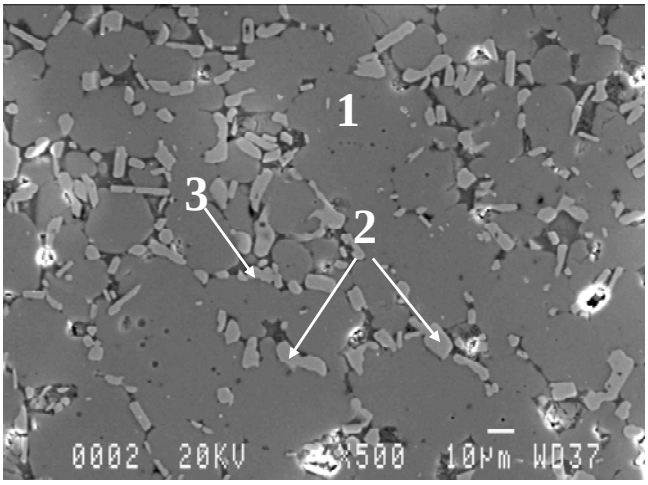

Fig. 10. SEM micrograph of the Ti_3Al-10 vol. % TiC composite with: (1) Ti_3Al grains in matrix, (2) a needle-like Ti_3AlC and (3) an Al-based phase.

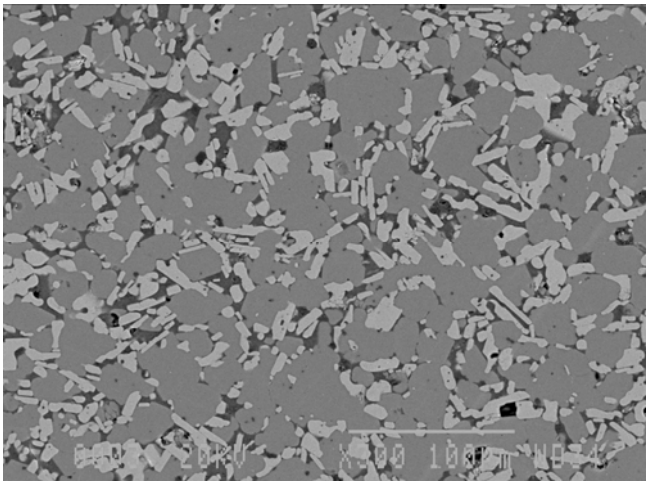

Fig. 11. Microstructure developed in Ti_3Al-20 vol. %TiC.

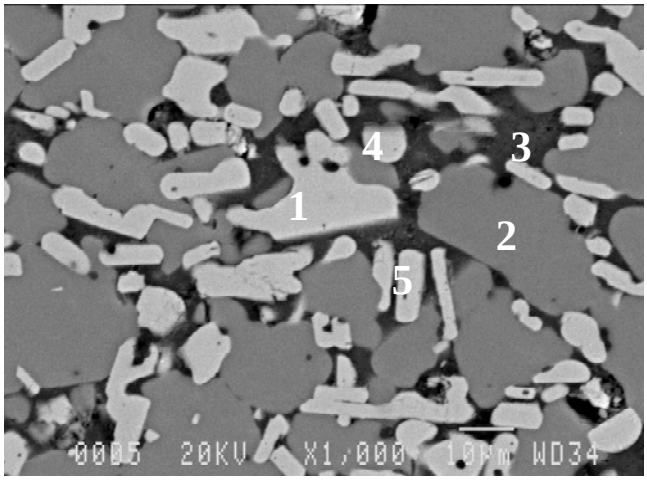

Fig.12. Individual phases in the microstructure of a Ti_3Al-20 vol.% TiC composite: (1) Ti-Al phase (2) Al_3Ti, (3) Al-based phase, (4) TiC and (5) Ti_2AlC.

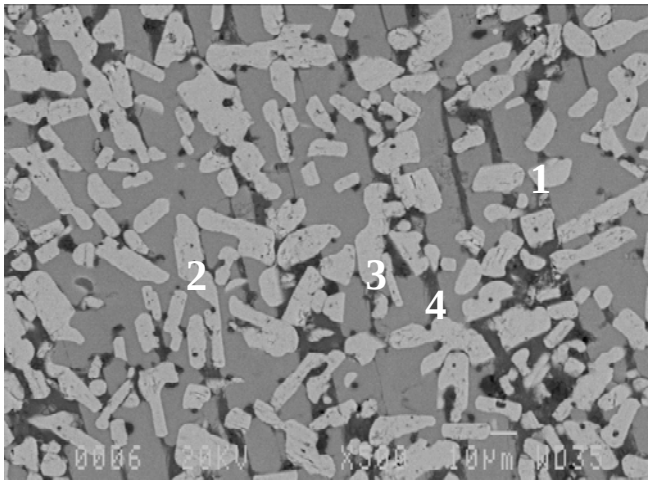

Fig.13: SEM micrograph of the TiAl-30 vol. %TiC composite.The individual phases are: (1) γ-TiAl and α_2-Al_3Ti colonies, (2) Ti-Al-C based grains, (3) Ti_3AlC and (4) Al-based phase.

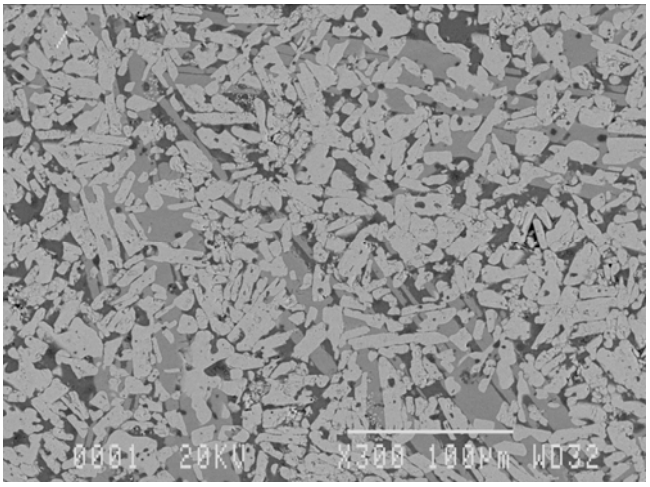

Fig.14. SEM micrographs of a fully dense Ti_3Al-40 vol. % TiC composite.

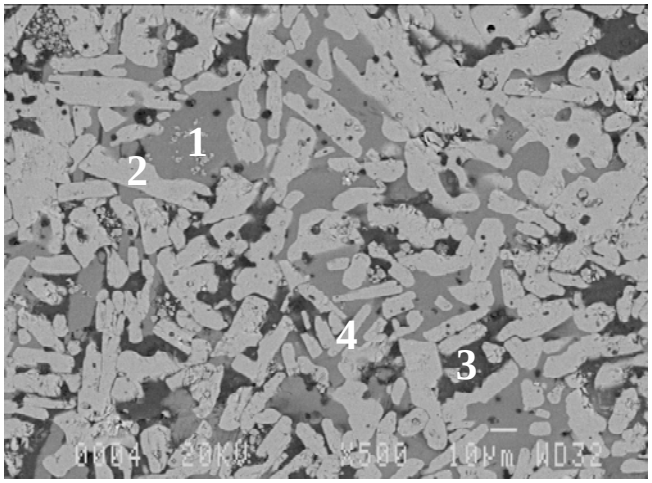

Fig.15. Individual phases in a fully dense Ti_3Al-40 vol. % TiC composite: (1) Ti_3Al, (2) Ti-Al-C based grains, (3) Ti_2AlC and (4) Al-based phase.

Mechanical properties

The results of room temperature tensile tests of composite samples are listed in Table 1. As a result of matrix reinforcement, significant improvements in Young's modulus, E,yield strength, 0.2YS, and ultimate tensile strength, UTS of the fabricated composites were observed, resulting in IMCs with excellent mechanical properties. These mechanical properties were found to be slightly higher in composites with an Ti_3Al-based matrix compared to TiAl-based matrix counterparts. At the same time, the highest improvement of strength caused by reinforcement was observed in samples reinforced with TiC and TiB_2 and less in samples reinforced with B_4C. Comparing the

mechanical properties of composite samples with various volume fractions of ceramic particles in the matrix, it was found that Young's modulus, yield strength and ultimate tensile strength increase while elongation decreases with an increasing fraction of ceramic reinforcement.

Table 1: Average room temperature tensile properties of various laboratory prepared composite samples

Initial chemical composition (vol. %)	Retained porosity (%)	E (GPa)	UTS (MPa)	0.2 % YS (MPa)	Elongation in 50 mm (%)
90% Ti_3Al + 10% TiB_2	1.4±0.1	268±25	721±70	442±40	0.8±0.08
90% Ti_3Al + 10% B_4C	1.2±0.1	257±25	698±70	397±40	0.7 ±0.07
90% Ti_3Al + 10% TiC	1.1±0.1	298±30	774±80	483±50	0.8±0.08
90% TiAl + 10% TiB_2	1.5±0.2	196±20	726±70	541±50	0.8±0.08
90% TiAl + 10% B_4C	1.4±0.1	192±20	698±70	518±50	0.7±0.07
90% TiAl + 10% TiC	1.4±0.1	208±20	739±70	573±60	0.8±0.08
80% Ti_3Al + 20% TiB_2	2.1±0.2	298±30	812±80	488±50	0.6±0.06
80% Ti_3Al + 20% B_4C	1.8±0.2	287±20	768±80	445±40	0.7±0.07
80% Ti_3Al + 20% TiC	1.9±0.2	335±20	868±90	549±50	0.5±0.05
80% TiAl + 20% TiB_2	2.3±0.2	238±25	798±80	593±60	0.6±0.06
80% TiAl + 20% B_4C	1.9±0.2	218±20	771±80	567±60	0.7±0.07
80% Ti_3Al + 20% TiC	1.9±0.2	236±25	819±80	622±60	0.7±0.07
70% Ti_3Al + 30% TiB_2	2.5±0.3	340±30	893±90	539±50	0.6±0.06
70% Ti_3Al + 30% B_4C	1.9±0.2	332±30	864±90	503±50	0.6±0.06
70% Ti_3Al + 30% TiC	2.1±0.2	351±35	947±90	589±60	0.6±0.06
70% TiAl + 30% TiB_2	3.0±0.3	281±40	901±90	641±60	0.5±0.05
70% TiAl + 30% B_4C	1.9±0.2	254±45	865±90	611±60	0.5±0.05
70% TiAl + 30% TiC	1.9±0.2	287±45	913±90	686±70	0.6±0.06
60% Ti_3Al + 40% TiB_2	3.1±0.3	376±45	997±100	598±60	0.4±0.04
60% Ti_3Al + 40% B_4C	1.8±0.2	368±45	994±100	564±60	0.5±0.05
60% Ti_3Al + 40% TiC	1.9±0.2	392±45	1022±100	648±60	0.3±0.03
60% TiAl + 40% TiB_2	3.6±0.4	318±45	988±100	699±70	0.4±0.04
60% TiAl + 40% B_4C	2.9±0.3	288±45	959±100	671±70	0.4±0.04
60% TiAl + 40% TiC	1.9±0.2	322±45	973±100	720±70	0.4±0.04
50% Ti_3Al + 50% TiB_2	4.2±0.4	440±45	1108±110	677±70	0.3±0.03
50% Ti_3Al + 50% B_4C	2.8±0.3	448±45	1105±110	658±70	0.3±0.03
50% Ti_3Al + 50% TiC	2.9±0.3	453±45	1129±110	704±70	0.3±0.03
50% TiAl + 50% TiB_2	5.1±0.5	402±45	1103±110	768±80	0.1±0.01
50% TiAl + 50% B_4C	2.8±0.3	397±45	1087±110	759±80	0.2±0.02
50% TiAl + 50% TiC	2.9±0.3	421±45	1116±110	799±80	0.1±0.01

Conclusion

A study of the fabrication of titanium aluminide-based intermetallic matrix composites (IMCs) discontinuously reinforced with various amounts (from 10 to 50 vol. %) of ceramic particles (B_4C, TiB_2 and TiC) was conducted by applying conventional pressureless reactive sintering of single phase titanium aluminide powders (TiAl or Ti_3Al) and ceramic reinforcement. In all systems and compositions, fully dense composite samples (with a retained porosity less than 1 vol. %) were successfully obtained, revealing the significant industrial potential of this fabrication method.

Qualitative metallographic analysis of the as-densified microstructures confirmed that during densification of the composite matrix both TiAl and Ti_3Al single phase titanium aluminide powders were transformed into various intermetallic phases (TiAl, Ti_3Al and $TiAl_3$). In addition, numerous secondary phases formed *in situ* by chemical reactions between titanium aluminide phases and the ceramic reinforcements were also identified.

In the case of a titanium aluminide matrix reinforced with B_4C, secondary phases formed in situ were TiB_2 and TiC, although traces of $AlB_{24}C_4$, Al_4C_3 and AlB_{12} were also confirmed.

In composite titanium aluminides reinforced with TiB_2 no appearance of secondary phases was found. However, intensive phase transformations occurred, particularly along the grain boundaries of the sintered titanium aluminide skeleton resulting in samples with planar grain boundaries and traces of various Ti_xAl_y phases.

The highest chemical reactivity and also sinterability was observed in TiAl-TiC and Ti_3Al-TiC samples.

Regarding the room temperature tensile properties, excellent yield strength, tensile yield strength and modulus were measured in all fully dense composite samples, irrespective of their phase composition and volume fraction of reinforcement. The best values were obtained in TiAl-TiC and Ti_3Al-TiC samples with the highest amount (50 vol. %) of ceramic reinforcement. Generally, the improvement of tensile strength, yield strength and modulus was found to correlate with the increase in the amount of ceramic reinforcement in the matrix. However, quite the opposite behaviour was found regarding elongation, where the introduction of ceramic particles into the intermetallic matrix led in all specimens to a significant reduction of elasticity.

Acknowledgment

This work was supported by funding from the Public Agency for Research and Development of the Republic of Slovenia, as well as the Impol Aluminium Company from Slovenska Bistrica, Slovenia, under contract No. 1000-07-219308

References

[1] *Gamma Titanium Aluminide 1999*, Y. W. Kim, D. M. Dimiduk, and M. H. Loretto, eds., TMS, Warrendale, PA, 1999, pp.3.

[2] S. Djanarthany, J. C. Viala, and J. Bouix, Mater. Chem. Phys., 72 (2001) 301.

[3] C. M. Ward-Close, R. Minor, and P. J. Doorbar: Intermetallics, 4 (1996) 217.
[4] P. C. Brennan, W. H. Kao, and J. M.Yang, Mater. Sci. Eng. A, 153 (1992) 635.
[5] J. C Rawers, and W. Wrzesinski, Scripta Met. & Mat., 24 (1990) 1985.
[6] H. Y. Sohn and X. Wang, J. Mater. Sci., 31 (1996) 3281.
[7] G. H. Wang and M. Dahms, Scripta Met. & Mat. 26 (1992) 1469.
[8] G. X. Wang, M. Dahms, G. Leitner, and S. Schultrich, J. Mater. Sci., 29 (1994) 1847.
[9] T. W. Lee and C. H. Lee, J. Mater. Sci. Lett., 17 (1998) 1367.
[10] G. X. Wang and M. Dhams, Powder Met. Int., 24 (1992) 219.
[11] G. Leitner, M. Dhams, W. Poeβnecker, and B. Wildhagen, in Proce. Int. Conf. on P/M Aerospace Materials 1991 (MPR Publishing Services Ltd, Shrewsbury, UK, 1992).
[12] F. J.J. Van Loo and G. D. Rieck, Acta Metall., 21 (1973) 61.
[13] M. Dahms, Mater. Sci. Eng. A, 110 (1989) 5.
[14] W. Misiolek and R. M. German, Mater. Sci. Eng. A, 144 (1991) 1.
[15] G. X. Wang and M. Dahms, Metall. Trans. A, 24 (1993) 1517.
[16] J. C. Rawers and W. R. Wrzesinski, J. Mater. Sci., 27 (1992) 2877.
[17] K. Taguchi, M. Ayada, K. N. Isihara, and P. H. Shingu, Intermetallics, 3 (1995) 91.
[18] H. E. Maupin and J. C. Rawers, J. Mater. Sci. Lett., 12 (1993) 165.
[19] H. E. Maupin and J. C. Rawers, *ibid.*, 12 (1993) 540.
[20] R. G. Rowe and S. C. Huang, *Israel J. Tech.*, 1988, vol.24, pp.255.
[21] K. S. Chan and Y. W. Kim, Met. Trans. A, 23 (1992) 1663.
[22] M. Grujicic and G. Cao, J. Mater. Sci., 37 (2002) 1.
[23] M. Sujata, S. Bhabgava and S. Sangal, J. Mater. Sci. Lett., 16 (1997) 1175.
[24] A. J. Pyzik and D. R. Beaman, J. Am. Ceram. Soc., 78 (1995) 305.
[25] J. Jung and S. Kang, *ibid.,* 87 (2004) 47.
[26] A. Banjeri and W. Reif, Metall. Trans. A, 17 (1986) 2127.